Proc. Natl. Acad. Sci. USA
Vol. 73, No. 10, pp. 3549–3553, October 1976
Biophysics

Kinetic evidence for hapten-induced conformational transition in immunoglobulin MOPC 460

(antibody function/chemical relaxation/allosteric mechanism)

DORON LANCET AND ISRAEL PECHT

Department of Chemical Immunology, The Weizmann Institute of Science, Rehovot, Israel

Communicated by Manfred Eigen, June 24, 1976

ABSTRACT **The kinetics of hapten binding to the homogeneous immunoglobulin A secreted by the murine plasmacytoma MOPC 460 was investigated by the chemical relaxation method. Two distinct relaxation times were observed in the binding equilibrium with three different haptens. A detailed concentration dependence analysis of relaxation times and amplitudes was performed with the hapten ε-*N*-(2,4-dinitrophenyl)-lysine (Dnp-Lys). The results support a mechanism in which two interconvertible conformational states of the protein bind the hapten with different association constants. Hapten binding shifts the equilibrium towards the better binding state. These observations form kinetic evidence for a conformational transition induced in the immunoglobulin by ligand binding to its antigen binding site, and are in line with the allosteric hypothesis for the initiation of physiological functions by antigen–antibody association.**

The binding of antigen to its specific site is known to induce several physiological activities at other remote sites on the antibody molecule. Conformationally mediated interaction (allostery) is one of the models proposed to account for this phenomenon (1). Evidence for such antigen-induced conformational transitions arose mainly from static measurements (1–3), while kinetic studies failed to resolve more than a single (association) step in hapten–immunoglobulin equilibria (4, 5). Here we report a study of the interaction between MOPC-460, a homogeneous immunoglobulin A, and its specific nitroaromatic haptens. This system has been previously characterized and shown to constitute an adequate model for antibody–antigen interaction (6–8). The method of chemical relaxation (9) was used to resolve the binding mechanism. Two relaxation times, of which one was bimolecular and the other monomolecular, were observed. The results form unequivocal kinetic evidence for protein isomerization in a hapten–immunoglobulin equilibrium.

MATERIALS AND METHODS

The reduced and alkylated protein 460 monomer was prepared from the ascites fluid of tumor-bearing BALB/c mice according to Goetzl and Metzger (10). Measurements were carried out in 0.01 M sodium phosphate buffer containing 0.15 M NaCl at pH 7.4. Temperature-jump experiments were done on an apparatus described elsewhere (11). The discharge voltage was 20 kV, causing a temperature jump of 5.2° from an initial temperature of 20.0 ± 0.1°. Concentration changes were monitored via the quenching of the protein intrinsic fluorescence by the haptens, and in the case of 4-(α-*N*-L-alanine)-7-nitrobenz-2-oxa-1,3-diazole (NBD-Ala, ref. 12) also through the quenching of the hapten fluorescence as well as changes in its absorption. Relaxation curves were converted into digital values with a Biomation model 802 transient recorder. Recordings were made at two different sweep rates and a sum of 6 to 8 jumps was used for the calculations. Relaxation times and amplitudes were fitted by the method of Grinvald and Steinberg (13). The observed amplitude ΔF_{obs} (in arbitrary units) depends on an amplification factor which may change from one concentration point to another, and is given by the general expression:

$$\Delta F_{obs} = \Sigma a_i \cdot \Delta F_i$$

where ΔF_i are molar fluorescence changes of the steps in the arbitrary units, and the coefficients a_i include equilibrium concentrations and molar enthalpies. To provide a consistent concentration dependence analysis, the amplitude is normalized by dividing the above equation by $P_t \cdot F_p$ (P_t is total protein concentration and F_p is the molar fluorescence of the protein in the arbitrary units). For each jump, the total fluorescence signal (F) at the high temperature equilibrium state is also measured at the same amplification. F is given by $F = F_p \cdot P_t \cdot (1 - q)$ where q is the fractional quenching of fluorescence at the particular hapten concentration, as obtained from titrations. The normalized amplitude is then given by:

$$A = \Delta F_{obs}(1 - q)/F = (1/P_t)\ \Sigma a_i \cdot \Delta f_i$$

and is independent of instrumental setting. The first expression contains only measurable quantities, and the second (in which $\Delta f_i = \Delta F_i / F_p$) is theoretical and yields the formulae in rows H and I of Table 1. The expressions for the concentration dependence of times and amplitudes were derived according to Castellan (14) and Jovin (15), respectively. The experimental concentration dependences were fitted to those predicted by different mechanisms using the algorithm of Powell (16).

RESULTS AND INTERPRETATION

Overall equilibrium parameters

Parameters were obtained by fluorometric titrations and calorimetric measurements which will be described in detail elsewhere. For ε-*N*-(2,4-dinitrophenyl)-L-lysine (Dnp-Lys) these were: overall association constant (compare Table 1) $K = 6.5 \pm 0.5 \times 10^4\ M^{-1}$; overall fluorescence change $\Delta f = -0.48 \pm 0.03$; and overall molar enthalpy change $\Delta H = -14.5 \pm 1.5$ kcal/mol; all are in agreement with ref. 7. The corresponding values for NBD-Ala were $K = 3.5 \pm 0.2 \times 10^5\ M^{-1}$, $\Delta f = -0.45 \pm 0.03$, and $\Delta H = -9.3 \pm 1.0$ kcal/mol (1 kcal = 4.184 kJ). The interaction of NBD-Ala with protein 460 and other Dnp-binding immunoglobulins will be fully described in a separate manuscript.

Temperature-jump experiments

The relaxation spectrum for the system of Dnp-Lys and protein 460 is composed of two relaxation times that are well separated over the whole concentration range. The concentration de-

Abbreviations: Dnp-Lys, ε-*N*-(2,4-dinitrophenyl)-L-lysine; NBD-Ala, 4-(α-*N*-L-alanine)-7-nitrobenz-2-oxa-1,3-diazole; τ_S, τ_F, slow and fast relaxation times; A_S, A_F, slow and fast normalized relaxation amplitudes.

Table 1. Possible mechanisms and their kinetic behavior

		1	2	3
A	MECHANISM	$H+T_0 \underset{k_{-T}}{\overset{k_T}{\rightleftharpoons}} T_1$; $k_{-1}\downarrow\uparrow k_1$; R_1	T_0; $k_{-0}\downarrow\uparrow k_0$; $H+R_0 \underset{k_{-R}}{\overset{k_R}{\rightleftharpoons}} R_1$	$H+T_0 \underset{k_{-T}}{\overset{k_T}{\rightleftharpoons}} T_1$; $k_{-0}\downarrow\uparrow k_0$; $k_{-1}\downarrow\uparrow k_1$; $H+R_0 \underset{k_{-R}}{\overset{k_R}{\rightleftharpoons}} R_1$
B	OVERALL ASSOCIATION CONSTANT	$K = K_T(1+K_1)$	$K = K_R/(1+K_0^{-1})$	$K = K_T(1+K_1)/(1+K_0)$
C	FAST TIME	$\frac{1}{\tau_F} = k_T(T_0+H)+k_{-T}$	$\frac{1}{\tau_F} = k_R(R_0+H)+k_{-R}$	$\frac{1}{\tau_{F1}} = k_T(T_0+H)+k_{-T}$; $\frac{1}{\tau_{F2}} = k_R\left(H+R_0\frac{1+K_TH}{1+K_T(H+T_0)}\right)+k_{-R}$
D	SLOW TIME	$\frac{1}{\tau_S} = k_1\frac{K_T(T_0+H)}{1+K_T(T_0+H)}+k_{-1}$	$\frac{1}{\tau_S} = k_{-0}\frac{K_RR_0+1}{K_R(R_0+H)+1}+k_0$	$\frac{1}{\tau_S} = \frac{k_0+k_1K_THX}{1+K_THX}+\frac{k_{-0}+k_{-1}K_RHY}{1+K_RHY}$; $X=\frac{T_0+R_0+H+K_R^{-1}}{K_TK_R^{-1}T_0+R_0+H+K_R^{-1}}$; $Y=\frac{T_0+R_0+H+K_T^{-1}}{T_0+K_RK_T^{-1}R_0+H+K_T^{-1}}$
E	$\lim_{H\to 0}\frac{1}{\tau_S}$	$k_1/(1+K_T^{-1}T_0^{-1})+k_{-1}$	k_0+k_{-0}	k_0+k_{-0}
F	$\lim_{H\to\infty}\frac{1}{\tau_S}$	k_1+k_{-1}	k_0	k_1+k_{-1}
G	$\underset{\sim}{g}$ MATRIX	$\begin{bmatrix}\frac{1}{T_0}+\frac{1}{T_1}+\frac{1}{H} & -\frac{1}{T_1}\\ -\frac{1}{T_1} & \frac{1}{T_1}+\frac{1}{R_1}\end{bmatrix}$	$\begin{bmatrix}\frac{1}{R_0}+\frac{1}{R_1}+\frac{1}{H} & -\frac{1}{R_0}\\ -\frac{1}{R_0} & \frac{1}{T_0}+\frac{1}{R_0}\end{bmatrix}$	$\begin{bmatrix}\frac{1}{T_0}+\frac{1}{T_1}+\frac{1}{H} & \frac{1}{H} & \frac{1}{T_0}\\ \frac{1}{H} & \frac{1}{R_0}+\frac{1}{R_1}+\frac{1}{H} & -\frac{1}{R_0}\\ \frac{1}{T_0} & -\frac{1}{R_0} & \frac{1}{T_0}+\frac{1}{R_0}\end{bmatrix}$
H	FAST AMPLITUDE	$A_F = \frac{1}{g_{11}P_t}\Delta f_T\,\Delta\ln K_T$	$A_F = \frac{1}{g_{11}P_t}\Delta f_R\,\Delta\ln K_R$	$A_{F1} = \frac{1}{g_{11}P_t}\Delta f_T\,\Delta\ln K_T$ $\quad Q_{12} = -\frac{g_{12}}{g_{11}}$; $A_{F2} = \frac{g_{11}}{\lvert\underset{\sim}{g}_2\rvert P_t}(Q_{12}\Delta f_T+\Delta f_R)(Q_{12}\Delta\ln K_T+\Delta\ln K_R)$
I	SLOW AMPLITUDE	$A_S = \frac{g_{11}}{\lvert\underset{\sim}{g}_2\rvert P_t}(Q_{12}\Delta f_T+\Delta f_1)\cdot(Q_{12}\Delta\ln K_T+\Delta\ln K_1)$; $Q_{12} = -\frac{g_{12}}{g_{11}}$	$A_S = \frac{g_{11}}{\lvert\underset{\sim}{g}_2\rvert P_t}(Q_{12}\Delta f_R+\Delta f_0)\cdot(Q_{12}\Delta\ln K_R+\Delta\ln K_0)$; $Q_{12} = -\frac{g_{12}}{g_{11}}$	$A_S = \frac{\lvert\underset{\sim}{g}_2\rvert}{\lvert\underset{\sim}{g}_3\rvert P_t}(Q_{13}\Delta f_T+Q_{23}\Delta f_R+\Delta f_0)\cdot(Q_{13}\Delta\ln K_T+Q_{23}\Delta\ln K_R+\Delta\ln K_0)$; $Q_{13} = \frac{1}{\lvert\underset{\sim}{g}_2\rvert}(g_{12}g_{23}-g_{13}g_{22})$ $\quad Q_{23} = \frac{1}{\lvert\underset{\sim}{g}_2\rvert}(g_{12}g_{13}-g_{11}g_{23})$

Formulae are referenced by the column number and the row letter.

Symbols denote species as well as their equilibrium concentrations: H, hapten; R_0 and R_1, free and bound protein in the better binding state; T_0 and T_1, free and bound protein in the worse binding state. P_t, total protein concentration.

The overall association constant is defined as $K = (R_1 + T_1)/H\cdot(R_0 + T_0)$. Individual equilibrium constants are defined as $K_i = k_i/k_{-i}$ and the direction of k_i is defined to be from reactants to products.

The associations are assumed to be much faster than the isomerizations. For mechanism 3 the association to the T state is assumed to be much faster than that to the R state (see *text*).

g_{ij} is the element of the matrix $\underset{\sim}{g}$ on the i-th row and j-th column. $\underset{\sim}{g}_i$ is the principal partial matrix of order i derived from $\underset{\sim}{g}$, and $|\underset{\sim}{g}_i|$ is its determinant.

$\Delta\ln K_i = \Delta H_i\Delta T/RT^2$, where ΔT is the temperature difference in the jump, ΔH_i is the molar enthalpy change of the i-th step, R is the gas constant, and T is the absolute temperature. Δf_i is the normalized molar fluorescence change of the i-th step (see *Materials and Methods*).

pendences of the fast time (τ_F) and slow time (τ_S) are shown in Fig. 1A and B, respectively. The protein concentration is held constant at about 1.6 μM (sites) and the reciprocal relaxation times are plotted versus the increasing total Dnp-Lys concentration (H_t). $1/\tau_F$ increases linearly from $1\cdot10^3$ to $4\cdot10^3$ sec^{-1}, while $1/\tau_S$ decreases from 120 sec^{-1} to a plateau value of about 50 sec^{-1}. This behavior is consistent with a reaction scheme that includes a fast bimolecular hapten–protein association and a slow monomolecular protein isomerization, most probably a conformational transition. The following observations confirm this tentative interpretation.

1. The fast association is kinetically and thermodynamically uncoupled from the slow isomerization. Also the hapten concentration is, to a good approximation, buffered (9) for all but the first three points of Fig. 2. Under these two conditions τ_F may be approximated by $1/\tau_F = k_{on}\cdot H_t + k_{off}$ independent of

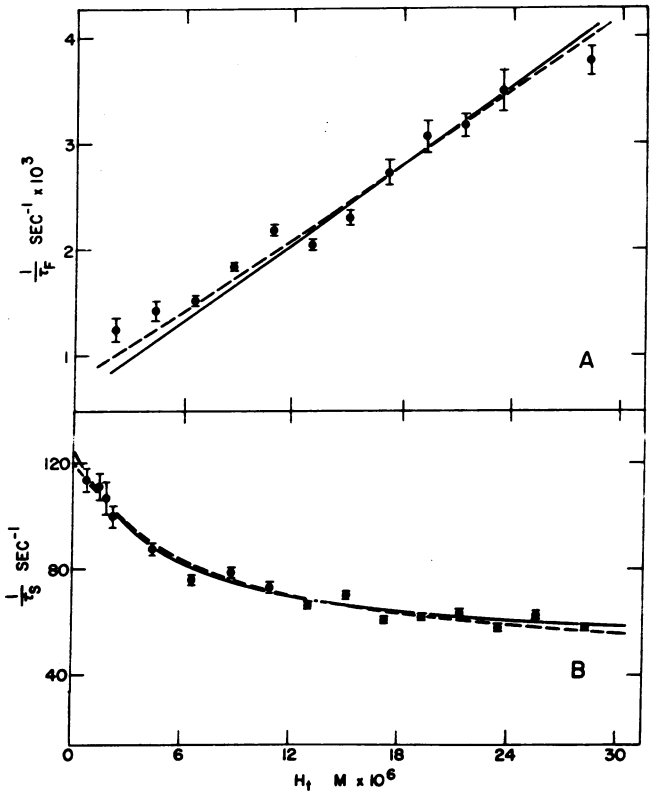

FIG. 1. The dependence of the inverse fast (A) and slow (B) relaxation times on total Dnp-lysine concentration. The broken and solid lines are calculated using the best fit parameters for mechanisms 2 and 3, respectively. The concentration of protein 460 was 1.5 – 1.7 μM sites. The bars denote approximate standard deviation in the group of jumps represented by one point.

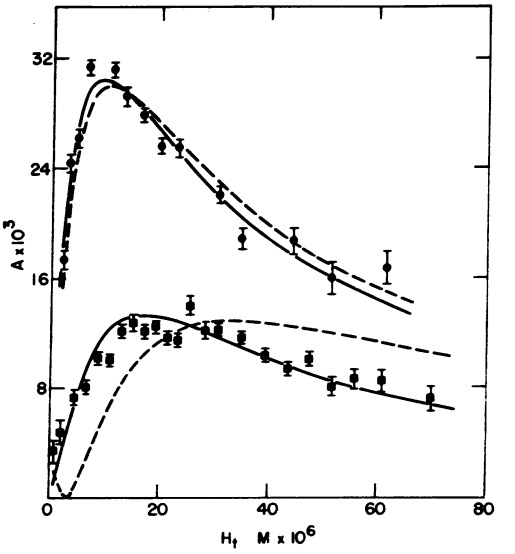

FIG. 2. The dependence of fast relaxation amplitude (upper curve) and slow relaxation amplitude (lower curve) on total Dnp-Lys concentration. The broken and solid lines are calculated using the best fit parameters for mechanisms 2 and 3, respectively. All other details are the same as in Fig. 1.

the detailed mechanism. (H_t is total hapten concentration and k_{on} and k_{off} are the rate constants for the association and dissociation, respectively.) The slope and intercept of a straight line drawn through the last nine points of Fig. 2 yield $k_{on} = 1.1 \times 10^8$ M^{-1} sec^{-1} and $k_{off} = 850$ sec^{-1}. The equilibrium constant characterizing the association step is $K_{ass} = k_{on}/k_{off} = 1.3 \times 10^5$ M^{-1}. The rate constants are similar to those found for other immunoglobulin–hapten systems (5) and the equilibrium constant is of the same order of magnitude as the overall constant from titrations, all in agreement with τ_F representing the hapten–protein association.

2. (*a*) Preliminary experiments with two other haptens, (NBD-Ala and 2,4-dinitronaphth-1-ol) were found to yield similar relaxation spectra with an identical limiting value for the slow time. τ_S must therefore be due to a common component of all three systems, namely the protein. (*b*) None of the free haptens displayed a chemical relaxation in any detection method. In contrast, the free protein exhibited in its intrinsic fluorescence a relaxation with $1/\tau = 110 \pm 30$ sec^{-1} and a normalized amplitude $A = 1.5 \pm 0.5 \times 10^{-3}$ which roughly agree with the extrapolation to $H_t = 0$ of $1/\tau_S$ and A_S, respectively (compare Figs. 1 and 2). This further confirms that the slow process is due to the protein.

3. Variation of the protein concentration from 1.6 to 30 μM at a constant hapten concentration did not change the value of τ_S. Also, no oligomeric forms higher than the monomer were found in sedimentation velocity measurements of both the free and Dnp-Lys-bound protein at a concentration of 60 μM sites. Thus, the possibility that τ_S reflects protein–protein association is excluded, and the slow step is proven to be monomolecular.

4. This monomolecular transition in the protein must be coupled to the binding of the hapten since: (*a*) τ_S is found to change with hapten concentration (Fig. 1). (*b*) In the case of NBD-Ala the slow time is observed not only in the protein fluorescence but also via changes in the hapten fluorescence and light absorption.

Two minimal mechanisms that conform with this scheme are 1 and 2 of Table 1. In mechanism 1 the protein–hapten complex isomerizes, while in mechanism 2 it is the free protein. Mechanism 1 is ruled out for the following reasons: (*i*) The decrease of $1/\tau_S$ with increasing hapten concentration is not compatible with Eqs. **1D**, **1E**, and **1F***. (*ii*) The kinetically determined K_{ass} is identified with K_T, and according to Eq. **1B**, $K \geq K_T$ must hold, in contrast with the observed $K < K_{ass}$. Mechanism 2 qualitatively agrees with the observed behavior, since Eqs. **2D**, **2E**, and **2F** predict a decreasing $1/\tau_S$, and $K_R = K_{ass} > K$ is consistent with Eq **2B**. An attempt is therefore made to examine its quantitative fit to all the data. In the fitting procedure the overall association constant (K), overall molar enthalpy change (ΔH), and maximal quenching (Δf) are fixed at the above measured values.

First, k_0 and k_{-0} are determined by fitting the slow time data (Fig. 1B) to Eq. **2D**. These are the only free parameters, since knowledge of k_0 and k_{-0} enables the calculation of K_0 ($=k_0/k_{-0}$) and K_R (using Eq. **2B** and the value of K). The fast time data (Fig. 1A) are then fitted to Eq. **2C** with k_R as the only free parameter (k_{-R} is calculated as k_R/K_R). The broken lines in Fig. 1 represent these respective fits and the resultant rate and equilibrium constants are listed in Table 2.

The relaxation amplitudes (Fig. 2) are then analyzed. The equilibrium constants obtained above are used to calculate the elements of the g matrix (Eq. **2G**) and the values of ΔH_i and Δf_i (molar enthalpy change and normalized fluorescence change of the i-th step, respectively) serve as free parameters.

* Equations denoted by a number and a letter appear in the corresponding column and row of Table 1.

Table 2. Kinetic and thermodynamic parameters for mechanisms 2 and 3

Mechanism	i	K_i	k_i	k_{-i}	Δf_i	ΔH_i	ΔG_i (f)	ΔS_i (g)
2	R	1.73×10^5 (b)	1.20×10^8 (a)	690 (a)	−0.48 (c)†	−15.9 (c)†	−7.12	−29.5
	0	0.56 (b)	43 (b)	77 (b)	—	—	—	—
3	T	1.90×10^4 (e)	1.3×10^8 *	6800 *	−0.47 (d)	−14.1 (d)	−5.81	−27.8
	R	2.18×10^5 (e)	1.27×10^8 (a)	580 (a)	−0.50 (d) §	−15.0 (d) §	−7.25	−26.0
	0	0.30 (e)	29 (e)	96 (e)	0.02 (d)	0.64 (d)	0.71	−0.23
	1	3.40 (e)	44 (e)	13 (e)	−0.01 (d)	−0.26 (d)	−0.72	1.55

Units: k_T and k_R, $\text{sec}^{-1}\ \text{M}^{-1}$; all other k_i, k_{-i}, sec^{-1}; K_T and K_R, M^{-1}; K_0, K_1, and Δf_i, dimensionless; ΔH_i and ΔG_i, kcal/mol; ΔS_i, cal/mol·degree. Error ± 20%.

Source of values: (a) τ_F, (b) τ_S, (c) A_F, (d) A_S, (e) τ_S and A_S, (f) by $\Delta G_i = RT\ln K_i$, (g) by $\Delta S_i = (\Delta H_i - \Delta G_i)/T$.

* According to the assumption $k_T = k_R$, see *text*.

† Only the product $\Delta H_R \Delta f_R$ is determinable and the listed values are obtained with the assumption $\Delta f_R = \Delta f$ (overall).

§ The fast amplitude fit yields a somewhat higher value for $\Delta H_R \cdot \Delta f_R$ (10.7 as compared with 7.5 kcal/mol here). This, however, corresponds to less than 20% difference in each of the two parameters within the estimated error.

The fast amplitude (Eq. **2H**) fits well (upper broke-line curve in Fig. 2) even though only the multiplying factor $\Delta f_R \cdot H_R$ is free and the shape of the curve is predetermined. In contrast, the slow amplitude (Eq. **2I**) does not give a satisfactory agreement, either when $\Delta f_R \cdot H_R$ is fixed to the value obtained above, or even when both Δf_R and ΔH_R are left free: in both cases the lower broken-line curve of Fig. 2 represents the best fit. Thus, mechanism 2 agrees with the behavior of three out of the four relaxation parameters, but is excluded by the slow amplitude data.

In view of this, a third mechanism (no. 3 in Table 1) is examined. Here both the free and the bound protein isomerize, and both the T and R forms bind the hapten with finite association constants ($K_R > K_T$ by definition). Only three of the four steps are thermodynamically independent, as reflected in the relation:

$$K_T/K_R = K_0/K_1 \qquad [4]$$

A maximum of three relaxation times may therefore be observed, and when the isomerizations are much slower than the associations (as borne out by experiment) one slow monomolecular time and two fast bimolecular times are expected (14). The slow time is unequivocally identified with the observed τ_S, and the data of Fig. 1B may thus be fitted to Eq. **3D**. Using the known value of K and Eq. **4**, four free parameters are left which are chosen as $q = k_0 + k_{-0}$, $p = k_1 + k_{-1}$, $r = k_0/k_1$, and $s = k_{-0}/k_{-1}$. This choice of parameters is decisive for successful convergence. Also, an initial guess for q and p is available according to Eqs. **3E**, and **3F**. While the values of the first three parameters are uniquely determined ($q = 125.5 \pm 1\ \text{sec}^{-1}$, $p = 52 \pm 2\ \text{sec}^{-1}$, and $r = 0.68 \pm 0.03$), s is found to be indeterminable in the sense that values from 2.8 through 10 yield the same fit (solid line in Fig. 1B). Even higher values up to $s = 60$ never give worse fit than the broken line of this figure ($s \to \infty$ corresponds to mechanism 2, see *Discussion*). Only when the slow relaxation amplitude is fitted to Eq. **3I** it is possible to resolve this degeneracy: the best fit is obtained with a value of $s = 7.4$ (lower solid-line curve in Fig. 2). The fit parameters (slow rate constants, all equilibrium constants and Δf_i, ΔH_i) are given in Table 2.

The fast relaxation data may now be treated in terms of two association steps having $K_T = 1.9 \cdot 10^4\ \text{M}^{-1}$ and $K_R = 2.2 \cdot 10^5\ \text{M}^{-1}$, respectively. τ_F may represent either one of the two expected fast times or a combination of both. To decide between these possibilities the fast amplitude is fitted to a total amplitude expression (cf. Eq. **20** of ref. 15) for a scheme that includes only the two ligand-coupled associations (time separation implies that during the fast relaxation the slow steps may be ignored). Computer simulations show that at the concentrations used and with the values of K_R and K_T, ligand-coupling is negligible and the total amplitude (A_T) assumes the form:

$$A_T = \frac{\Delta f_T \cdot \Delta \ln K_T}{g_{11} \cdot P_t} + \frac{\Delta f_R \cdot \Delta \ln K_R}{g_{22} \cdot P_t}$$

The first and second terms are the independent amplitude expressions for the associations to the T and R states, respectively, and have different functional shape. The attempted fit shows that the functional shape of the experimental fast amplitude is very close to that of a pure second term, indicating that the fast relaxation represents solely the association to the R state. The observed τ_F and A_F may thus be identified with τ_{F_2} and A_{F_2} (Table 1), respectively, and the corresponding fits yield the full line in Fig. 1A and the upper full line in Fig. 2 with the parameters listed in Table 2 (see note § of this table). Assuming that k_R and k_T are essentially diffusion controlled and therefore have similar values (cf. ref. 5), τ_{F_1} is expected to be shorter than τ_{F_2} by the factor $K_R/K_T \cong 10$. Attempts to resolve a second fast relaxation time shorter than 100 μsec lead to inconclusive results due to experimental difficulties. Nevertheless, mechanism 3 appears to be the simplest scheme that is consistent with the behavior of all the observable relaxation parameters.

In preliminary experiments with the Fab fragment the same relaxation spectrum was observed. The values and the general concentration dependence of the relaxation times were similar to those obtained with the intact protein. Still, the possibility of a quantitative difference in the relaxation behavior was not excluded. Similar relaxation phenomena were also observed in a non-reduced and alkylated preparation which contained the oligomeric forms of protein 460.

DISCUSSION

The assignment of mechanism 3 to the reaction of protein 460 with haptens is significant in two ways: (a) Hapten binding to an immunoglobulin is kinetically found to involve a conformational transition. The implications of this finding for the understanding of antibody function are discussed below. (b) It is an unequivocal kinetic assignment of mechanism 3 to an experimental system. This mechanism forms the basic element of the generalized allosteric scheme proposed by Eigen (17), and is actually the model of Monod, Wyman, and Changeux (18), as applied to an "allosteric monomer" ($n = 1$). On the other

hand, it includes the kinetically simpler mechanisms of Table 1 as limiting cases with $K_R \to \infty$, $K_0 \to 0$, for mechanism 1, and $K_T \to 0$, $K_1 \to \infty$ for mechanism 2. The studied system may therefore serve also as a useful model for ligand–protein interactions in general.

The results of this study show that when only relaxation times are considered, the data may be consistent with a whole range of parameters for mechanism 3, including the limit of one of the simpler mechanisms. All three mechanisms of Table 1 may thus be taken as different numerical cases of one thermodynamically general scheme. Analysis in terms of this scheme, using relaxation amplitudes in addition to relaxation times to resolve the appropriate set of parameters, seems therefore advisable.

The relative simplicity of mechanism 3 enables its full kinetic and thermodynamic characterization without simplifying assumptions (Table 2). The value of $K_T/K_R = K_0/K_1$ (c in the Monod–Wyman–Changeux formalism) is found to be 0.088. The difference between k_0 and K_1 is mostly due to a difference between k_{-0} and k_{-1} ($s = k_{-0}/k_{-1} = 7.4$), while k_0 and k_1 are only slightly different ($r = k_0/k_1 = 0.66$). This result resembles the situation previously introduced as an assumption (19), namely, that the rate constants for all T_t to R_t isomerizations in an allosteric oligomer are equal.

A value of $\Delta(\Delta G) = \Delta G_R - \Delta G_T = 1.4$ kcal/mol is calculated from Table 2. This difference in free energy of binding to the states T and R is due to roughly equal and relatively small enthalpic and entropic contributions. The two states of the protein are thus seen to have quite similar interactions with the hapten. Still, the value of $\Delta(\Delta G)$ (also equal to $\Delta G_1 - \Delta G_0$) is sufficient to invert the position of the conformational equilibrium: $\bar{R}$, the state function (18), changes from $K_0/(1 + K_0) = 0.23$ to $K_1/(1 + K_1) = 0.78$ with hapten saturation. This is possible since ΔG_0 is only +0.7 kcal/mol, corresponding to $L = 1/K_0 = 3.3$ in the Monod–Wyman–Changeux notation.

The hapten-induced conformational transition in protein 460 is consistent with the allosteric model for the initiation of physiological events by antigen–antibody complexes. This model assumes conformationally mediated heterotropic interactions between the antigen-binding site and effector sites in other domains of the antibody (1, 2). For immunoglobulins of the M class this is assumed to be sufficient, presumably since their pentameric structure eliminates the necessity for aggregation (1, 20). Protein 460, an immunoglobulin of the A class, is also oligomeric in its native form, and may behave similarly. It is noteworthy that antigen binding to immunoglobulin A is known to trigger the alternative complement pathway via a site on the Fab region (21), in line with the observed similarity of the relaxation behavior between the Fab fragment and the intact monomer or oligomer.

The binding of low-molecular-weight haptens to immunoglobulins is rarely found to have a physiological outcome, or to induce conformational phenomena. It seems that the physiologically active state of the immunoglobulin is attained via a major conformational change (ΔG_0 large and positive), which involves many residues in the antigen-binding site and probably has to do with the relative position of the light and heavy chains (2). $\Delta(\Delta G)$ for the binding of a small hapten may usually be insufficient to compensate for this large ΔG_0. Protein 460 may be a case where ΔG_0 is small, or where the pathway towards the full transition includes a conformational intermediate with a small ΔG_0. As a result, hapten-binding studies in this well-defined model system are able to yield at least partial information about the dynamics and energetics of the postulated antigen-induced conformational transition.

We thank Dr. M. Eigen, Dr. T. Jovin, and Dr. R. Rigler for their invaluable advice in theoretical and experimental matters. We are also indebted to Y. Blatt and M. Goldberg for reviewing this manuscript and R. Zhidovetsky for carrying out the calorimetric measurements.

1. Metzger, H. (1974) *Adv. Immunol.* **18**, 169–207.
2. Schlessinger, J., Steinberg, I. Z., Givol, D., Hochman, J. & Pecht, I. (1975) *Proc. Natl. Acad. Sci. USA* **72**, 2775–2779.
3. Pilz, I., Kratky, O., Licht, A. & Sela, M. (1975) *Biochemistry* **14**, 1326–1333.
4. Froese, A. & Sehon, A. H. (1975) *Contemp. Top. Mol. Immunol.* **4**, 23–54.
5. Haselkorn, D., Friedman, S., Givol, D. & Pecht, I. (1974) *Biochemistry* **13**, 2210–2222.
6. Jaffe, B. M., Simms, E. S. & Eisen, H. N. (1971) *Biochemistry* **10**, 1693–1699.
7. Johnston, M. F. M., Barisas, B. G. & Sturtevant, J. M. (1974) *Biochemistry* **13**, 390–396.
8. Rosenstein, R. W. R., Musson, R. A., Armstrong, M. Y. K., Konigsberg, W. H. & Richards, F. F. (1972) *Proc. Natl. Acad. Sci. USA* **69**, 877–881.
9. Eigen, M. & De Maeyer, L. (1974) in *Techniques of Chemistry*, ed. Weissberger, A. (John Wiley & Sons, New York), Vol. VI, part II, pp. 63–146.
10. Goetzl, E. J. & Metzger, H. (1970) *Biochemistry* **9**, 1267–1278.
11. Rigler, R., Rabl, C. R. & Jovin, T. M. (1974) *Rev. Sci. Instrum.* **45**, 580–588.
12. Gosh, P. B. & Whitehouse, M. W. (1968) *Biochem. J.* **108**, 155–156.
13. Grinvald, A. & Steinberg, I. Z. (1974) *Anal. Biochem.* **59**, 583–598.
14. Castellan, G. W. (1963) *Ber. Bunsenges. Phys. Chem.* **67**, 898–908.
15. Jovin, T. M. (1975) in *Biochemical Fluorescence: Concepts*, eds. Chen, R. F. & Edelhoeh, H. (Marcel Dekker Inc., New York), Vol. 1, pp. 305–374.
16. Powell, M. J. D. (1971) in *Harwell Subroutine Library*, Atomic Energy Research Establishment, Harwell, U.K. (subroutine VAOYA).
17. Eigen, M. (1968) in *Fast Reactions and Primary Processes in Chemical Kinetics*, ed. Claesson, S. (Almqvist and Wiksel, Stockholm), pp. 333–364.
18. Monod, J., Wyman, J. & Changeux, J. P. (1965) *J. Mol. Biol.* **12**, 88–118.
19. Kirschner, K., Eigen, M., Bittman, R. & Voigt, B. (1966) *Proc. Natl. Acad. Sci. USA* **56**, 1661–1667.
20. Brown, J. C. & Koshland, M. E. (1975) *Proc. Natl. Acad. Sci. USA* **72**, 5111–5115.
21. Götze, O. & Müller-Eberhard, J. (1971) *J. Exp. Med.* **134**, 90S–108S.